

Constraining BAO parameter with Bispectrum clustering of DESI Tracers

Mehdi Rezaie¹, Jayashree Behera¹, Lado Samushia¹ et al.

¹*Department of Physics, Kansas State University, 116 Cardwell Hall, Manhattan, KS 66506, USA*

Accepted XXX. Received YYY; in original form ZZZ

ABSTRACT

We use AbacusSummit simulations to explore the possibility of measuring the Baryon Acoustic Oscillation signal from the bispectrum of DESI (Dark Energy Spectroscopic Instrument) galaxies. We measure isotropic BAO from mock galaxy catalogs designed to replicate the various DESI samples. We use several methods to separate the BAO signal from the bispectrum, estimate the covariance of the measurements, and fit the distance scale to it. We show that the BAO signal in the bispectrum can significantly improve the distance constraints compared to the power spectrum alone analysis. **We will quote some numbers here once we have stable results.**

Key words: Awesome keywords: Perfect

1 INTRODUCTION

As a stage IV galaxy redshift survey, the Dark Energy Spectroscopic Instrument (DESI) utilizes 5000 robotically-driven fibers to simultaneously collect spectra of thousands of galaxies and quasars (?). Over its five-year mission, DESI will yield an unparalleled volume of spectra to construct the biggest 3D volume of the Universe, which can be leveraged to deepen our understanding of the formation and evolution of structures in the Universe, and most importantly, to shed light on the nature of dark energy (?).

Common clustering statistics for extracting information from data of galaxy redshift surveys, like DESI, are the power spectrum and two-point correlation function, which characterize the excess probability of finding two galaxies separated by a given wavenumber and distance, respectively, relative to a random distribution of galaxies. One of the primary features imprinted in the large-scale clustering of galaxies is Baryon Acoustic Oscillations (BAO), which are created by sound waves propagating through the early Universe before the epoch of recombination, i.e. when photons no longer were able to re-ionize atoms. These acoustic waves leave a characteristic scale in the distribution of galaxies that can be used as a standard ruler to measure distances in the Universe (see, e.g., ???).

In galaxy redshift surveys, the position of galaxies is measured via their redshifts, which is not a direct measurement of their true distances, but rather influenced by their peculiar velocities, i.e., the velocities of the galaxies relative to their local environment. These peculiar velocities can smear out the BAO feature by causing the distribution of galaxies to appear elongated along the line-of-sight direction. Additionally, non-linearities caused by subsequent structure formation impact the sharpness of the BAO signal and effectively reduce the statistical precision of the distance scale mea-

surements. Several reconstruction techniques have been developed to account for the smearing effect of BAO and recover the constraining power lost due to bulk flows and space distortions (see, e.g., ?). However, even with reconstruction techniques applied, cosmic variance imposes a limitation on the amount of information that can be extracted from the two-point statistics of the large-scale structure. Cosmic variance can be reduced by increasing the size of the survey volume via either surveying a larger area of the sky or by going deeper in redshift.

Measuring the correlation between triplets (or even quadruplets) of galaxies is an alternative way of accessing extra information that is independent of the one in the two-point statistics. The analysis of higher-order statistics from real data has so far resulted in moderate improvements in the cosmological constraints. The high-density DESI galaxy samples may perform significantly better. The standard ruler-based probes (such as the BAO) could, at least in principle, perform better than the reconstructed fields Samushia et al. (2021).

Recent developments in algorithms utilizing rotational symmetries and advancements in computing power have made higher-order statistics more feasible to measure (see, e.g., ??????). Higher order clustering measurements have been used to improve parameter constraints or break parameter degeneracies on modified theories of gravity (?), galaxy-halo connections (?), cosmic distance scales (?), and baryon-dark matter relative velocity (?).

DESI is expected to deliver extremely precise measurements of galaxy bispectrum from all its samples. To robustly analyze the data at the level of DESI statistical errors will require overcoming multiple theoretical challenges. The precision matrices for the bispectrum are difficult to accurately estimate from the mock catalogs

due to the large size of the data vector. The perturbation-theory-based methods for the bispectrum have been shown to break down on relatively large scales.

In this work, we explore the possibility of measuring and analyzing the BAO feature in the average (angular monopole) bispectrum. Even though the BAO feature extends to a higher wavenumber, the beat frequency is a large-scale feature set by linear physics in the early Universe. There is a hope that the extracted BAO frequency can be made unbiased even when the models for the full shape of the galaxy bispectrum fail to predict it with the desired accuracy.

Not having accurate covariance matrices for our measurements hinders our ability to directly interpret our likelihood surfaces. We use a number of indirect methods to assess the variance in the measurement of the BAO scale from the bispectrum compared to the power spectrum. Some of these methods rely on artificially constructed covariance matrices that are conservative estimates of the true covariance. Other methods estimate the variance by looking at the spread of BAO scale measurements over multiple mock catalogs.

Our preliminary findings are encouraging. The BAO feature is clearly visible in the measured bispectrum. A significant fraction of this signal does not seem to be strongly correlated with the same signal in the power spectrum. **We will put here some specific numbers once we have stable results.**

In this paper, we utilize simulations of galaxies with similar clustering properties as the DESI targets to characterize the constraining power on cosmic distance scales from the bispectrum. The outline of this paper is as follows. We discuss the templates for BAO power spectrum and bispectrum in Section A, and the details of simulations in Section 3. Finally, we present the constraints in 6, and conclude with discussion and conclusion in 7.

2 SIMULATIONS

To assess the nature of the BAO signal in the DESI bispectrum we use *FirstGen* simulations. These simulations are based on *AbacusSummit* N-body simulations. The halos in the *AbacusSummit* have been populated with galaxies using the **we will describe how the FirstGens were produced here**. These HOD parameters were derived by fitting the projected small-scale clustering of the DESI Early Data Release sample.

We use *Molino* simulations to assist in constructing covariance matrices. *Molino* simulations are based on the *Quijote* N-body simulation suit. They were constructed by **Same thing here**.

We use the *GLAM* simulations for constructing some of our BAO fitting templates. **we will describe the volume the number, etc.** Each instance of the *GLAM* simulations was run with a paired simulation with no input BAO signal.

Molino (15,000 Mocks): $\Omega_M = 0.32$, $\sigma_8 = 0.834$, Volume $\sim 1\text{Gpc}/h^3$ Galaxy catalogs from the *Quijote* N-body simulations (Villaescusa-Navarro et al.2020) with the standard Halo Occupation Distribution model from Zheng et al. (2007). HOD parameters are based on high luminosity SDSS samples. More at changoonhahn.github.io/molino

And two other series of mocks provided by our DESI collaborators: *GLAM* (1,000 Mocks)

Abacus (25 mocks)

We estimate the reduced covariance matrix from a suite of 15000 simulations (*MOLINO*) and scale it by the variance of power spectrum or bispectrum for the *GLAM* or *ABACUS* realizations.

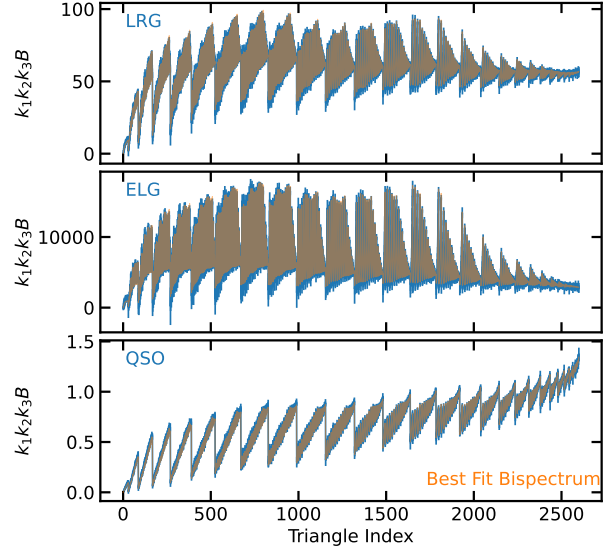


Figure 1. Mean bispectrum of the Abacus LRG, ELG, and QSO simulations, respectively, from top to bottom.

3 DESI MEASUREMENTS

We measure bispectrum using standard techniques described in . We start by dividing the cubic volume of simulations into $N_g \times N_g \times N_g$ sized three-dimensional grid, where $N_g = 1024$.

LS: I will put a description of the entire algorithm here later. Also here we should describe the triangular index and the kinds of reductions that we do.

We separate the bispectrum into smooth and BAOonly parts similar to how it's done for the power spectrum. We find functions B_{smooth} , and B_{BAO} such that

$$B = B_{\text{smooth}} B_{\text{BAO}}. \quad (1)$$

B_{smooth} models the bispectrum with the BAO signature removed. Even though its meaning is clear, it can not be rigorously defined from the first principles, which makes the separation into the smooth and BAO components part of the modeling. For a useful extracting we want the B_{BAO} component to be oscillating around 1 and decay at higher wavenumbers. By constraining ourselves to the BAO-only analysis we are hoping that while our models for the B_{smooth} may fail, the same models for the B_{BAO} component will remain accurate.

Points on figure 1 show the bispectrum of *FirstGen* mocks as a function of the triangular index. The error bars are estimated from the variance of the 25 *FirstGen* mocks for each tracer. The lines are the best-fit models from the leading order perturbation theory model (see Behera et al in prep), where the cosmological parameters have been fixed to the true values of the mocks and bias parameters were allowed to freely vary. The ELG tracers show the strongest clustering signal while the QSO sample show the weakest clustering signal which is dominated by shotnoise on small scales (large triangle indices).

Figure 2 shows the same measurements but divided by the smooth part of the bispectrum. **We will describe here what we see. Does the extraction always work well? high k problems?.** Figures 3 show the reduced measurements for the B_{BAO} .

Figure 4 shows the BAO-only power spectrum from the same simulations.

Figure 5 shows the bin-by-bin correlation of the bispectrum and power spectrum measurements.

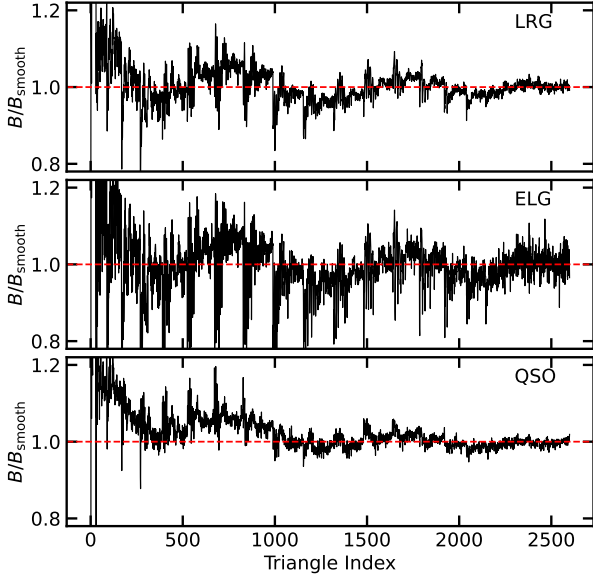


Figure 2. Same as Figure 1 for the ratio of bispectrum to smooth bispectrum.

4 MODELING THE BAO

To simplify our analysis, we assume isotropic dilution of the BAO scale. For the power spectrum,

$$P_t(k|\alpha, \nu) = \nu_0 P_r(\alpha k) + \nu_1 + \nu_2 k + \nu_3/k + \nu_4 k^2 + \nu_5/k^2, \quad (2)$$

where P_r is the ratio of the power spectrum to the BAO-less power spectrum. For the bispectrum, we have two extra degrees of freedom, namely k vs k_1, k_2, k_3 . We have,

$$\begin{aligned} \mathbf{B}_t(k_1, k_2, k_3|\alpha\nu) = & \nu_0 B(\alpha k_1, \alpha k_2, \alpha k_3) + \nu_1 + \nu_2(k_1 + k_2 + k_3) \\ & + \nu_3(1/k_1 + 1/k_2 + 1/k_3) \\ & + \nu_4(k_1 k_2 + \text{cycl}) + \nu_5[1/(k_1 k_2) + \text{cycl}] \\ & + \nu_6(k_1 k_2/k_3 + \text{cycl}) + \nu_7(k_3/(k_2 k_1) + \text{cycl}) \end{aligned} \quad (3)$$

We marginalize over the nuisance parameters using MCMC package called *emcee* and flat priors are imposed on all parameters including α .

5 COVARIANCES

We fit the BAO-only bispectra in *AbacusSummit* by minimizing the weighted squared difference between the measurements and the model,

$$\chi^2(\alpha, \nu) = \Delta \mathbf{B}^T \mathbf{W} \Delta \mathbf{B}, \quad (4)$$

where

$$\Delta \mathbf{B}(\alpha, \nu) = \mathbf{B}_m - \mathbf{B}_t(\alpha, \nu), \quad (5)$$

is the difference between measured and theoretical bispectra and \mathbf{W} is a positive definite weighting matrix that upweights the contribution of some linear combinations of $\Delta \mathbf{B}$ to the χ^2 compared to the others. The theoretical bispectrum depends on the BAO scale parameter α as well as nuisance parameters ν . We expect the χ^2 to achieve its minimum value at the true parameter α^* as long as our model is unbiased and the average value of $\Delta \mathbf{B}$ over many realizations is zero. The actual minimizer values $\hat{\alpha}$ from individual

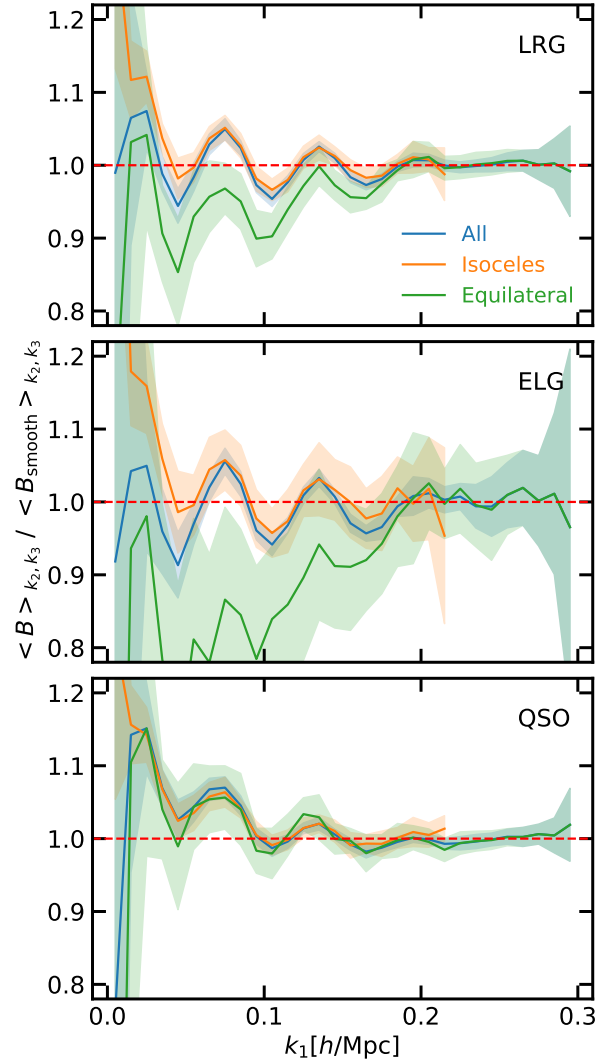


Figure 3. Same as Figure 2 for the reduced bispectrum.

realizations will be spread around the true value α^* with some standard deviation σ_α^* . We will estimate σ_α^* from the standard deviation of $\hat{\alpha}$ values - $\hat{\sigma}_\alpha$ - that we get from 25 *AbacusSummit* mocks. The fractional variance in our estimate of the error is expected to be

$$\frac{\text{Std}(\hat{\sigma}_\alpha)}{\sigma_\alpha^*} = \sqrt{\frac{2}{N_{\text{sample}} - 1}}. \quad (6)$$

$N_{\text{sample}} = 25$ in our case which results in a 28 percent uncertainty. The *AbacusSummit* boxes cover 8 cubic Gigaparsecs of volume which is significantly larger than the BAO scale. We expect the errors on the $\hat{\alpha}$ to scale as V^{-1} for larger volumes.

The main purpose behind the weighting matrix \mathbf{W} is to minimize σ_α^* by upweighting bispectrum combinations that are measured more precisely compared to the noisy ones. The optimal weighting is achieved when

$$\mathbf{W} = \mathbf{C}^{-1}, \quad (7)$$

where \mathbf{C}^{-1} is the true inverse covariance of the bispectrum measurements. Another convenient property of the weights following Eq. (7) is that when they are used the distribution of the α values in the Markov Chain Monte Carlo (MCMC) follows their true likelihood.

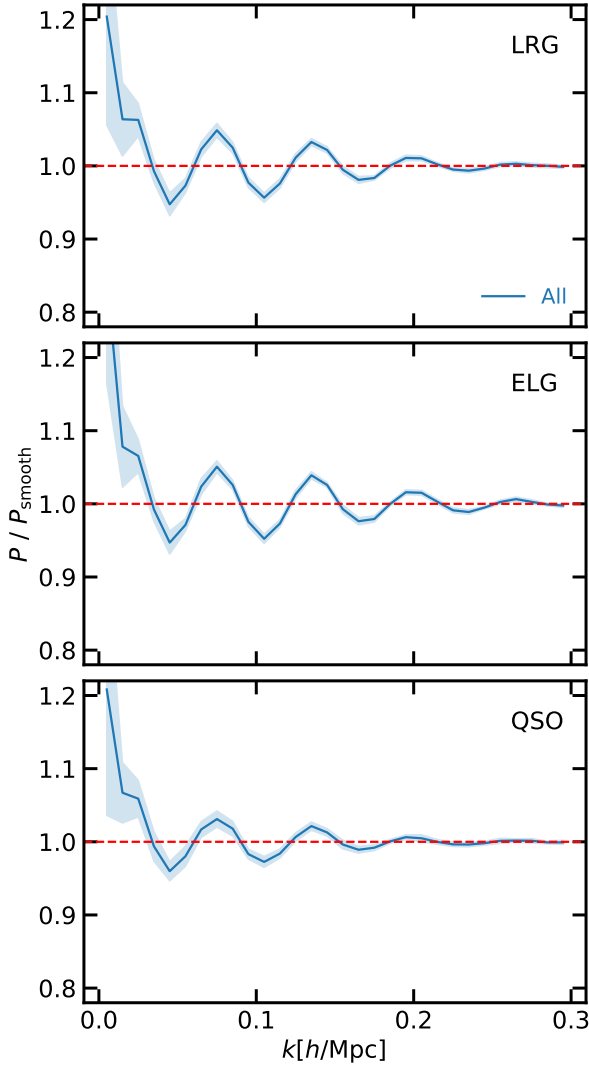


Figure 4. The ratio of the mean power spectrum to the mean smooth power spectrum.

This means that we can use the MCMC posterior distribution to estimate the error on our measurement of α which is more accurate than estimating it from a sample variance of a retrieved parameter from a small number of mocks, in which case the knowledge of the error on the measurement is limited by Eq. (6) (see, e.g., ?, for a comparison of two ways of estimating errors when combining BAO measurements.)

Unfortunately, at this point in time, we do not have a large suite of high-fidelity simulations for estimating accurate inverse covariance of our bispectrum measurements. Instead, we try a few different options for the weighting matrix based on the theoretical expectation of how the bispectrum variance is expected to scale for Gaussian fields (???).

We try out three weighting schemes in our analysis

- Diagonal errors from AbacusSummit simulations
- Correlated (non-diagonal) weighting from Molino simulations
- And a theoretically computed weighting based on a simple Gaussian model with shot-noise

The diagonal errors are computed by simply looking at the variance of each bispectrum mode and ignoring cross-correlations.

The resulting \mathbf{W} is diagonal which makes it numerically inexpensive to implement in our codes. Since this weighting scheme ignores cross-correlations between the modes and is based on a very small number of simulations, we don't expect it to be very optimal. We do expect it to provide us with a rough scaling between low and high wavenumber modes of the bispectrum. The fact that this weighting is derived from a significantly smaller number of mocks than the bispectrum modes that we use in our analysis is not a big problem for us since we are using Eq. (6) to estimate our errors. Even though we use MCMC to find $\hat{\alpha}$ values, we do not try to interpret the width of the MCMC posterior as our posterior likelihood and the usual problems associated with numerical inverse covariance matrices and Hartlap factors (????) do not apply to our analysis.

To get a sense of how the correlations between different bispectrum modes may affect the weighting we compute a reduced covariance matrix from 15,000 Molino simulations. The high number of simulations makes the coefficients of the reduced covariance matrix highly accurate. These cross-correlation coefficients give us some idea of how much the bispectrum modes measured from massive galaxies at lower redshifts can be correlated. We rescale this reduced covariance matrix by the standard diagonal errors described in the previous paragraph to get a weighting that accounts for the relative noise at different wavenumbers and the covariance between different wavenumbers at the same time.

Finally, we estimate the inverse covariance matrix of bispectrum measurements theoretically based on the expectation from purely Gaussian fields and accounting for Poisson shot noise and use it as our weight. This estimate is going to be off at higher wavenumbers where the non-Gaussian effects will diverge from our computations, but we still expect this weighting to be close to optimal and get the correct relative weighting between small wavenumbers that are dominated by cosmic variance and large wavenumbers that are dominated by shot noise.

LS: once we have all results we will write a sentence here summarizing our findings. Which weightings resulted in a tighter distribution of $\hat{\alpha}$.

6 BAO FITS

one or two options for the model. nuisance parameters.

Glam template. Linear template.

spread of measured alpha over 25 FirstGens

alongside with alpha fits to the power spectrum

experiment with some choices.

sigma alpha from the posterior (as a function of k)

min χ^2 vs alpha for P(k), B(k1, k2, k3), P+B BAO and BAOless templates. Look into the scatter in the detection significance across the realizations.

Below we summarize the mean of the posterior mean estimates, standard deviation, and 4-th and 96-th quantiles from simulations.

7 CONCLUSION

Where you provide the take-home message.

REFERENCES

Samushia L., Slepian Z., Villaescusa-Navarro F., 2021, Monthly Notices of the Royal Astronomical Society, 505, 628

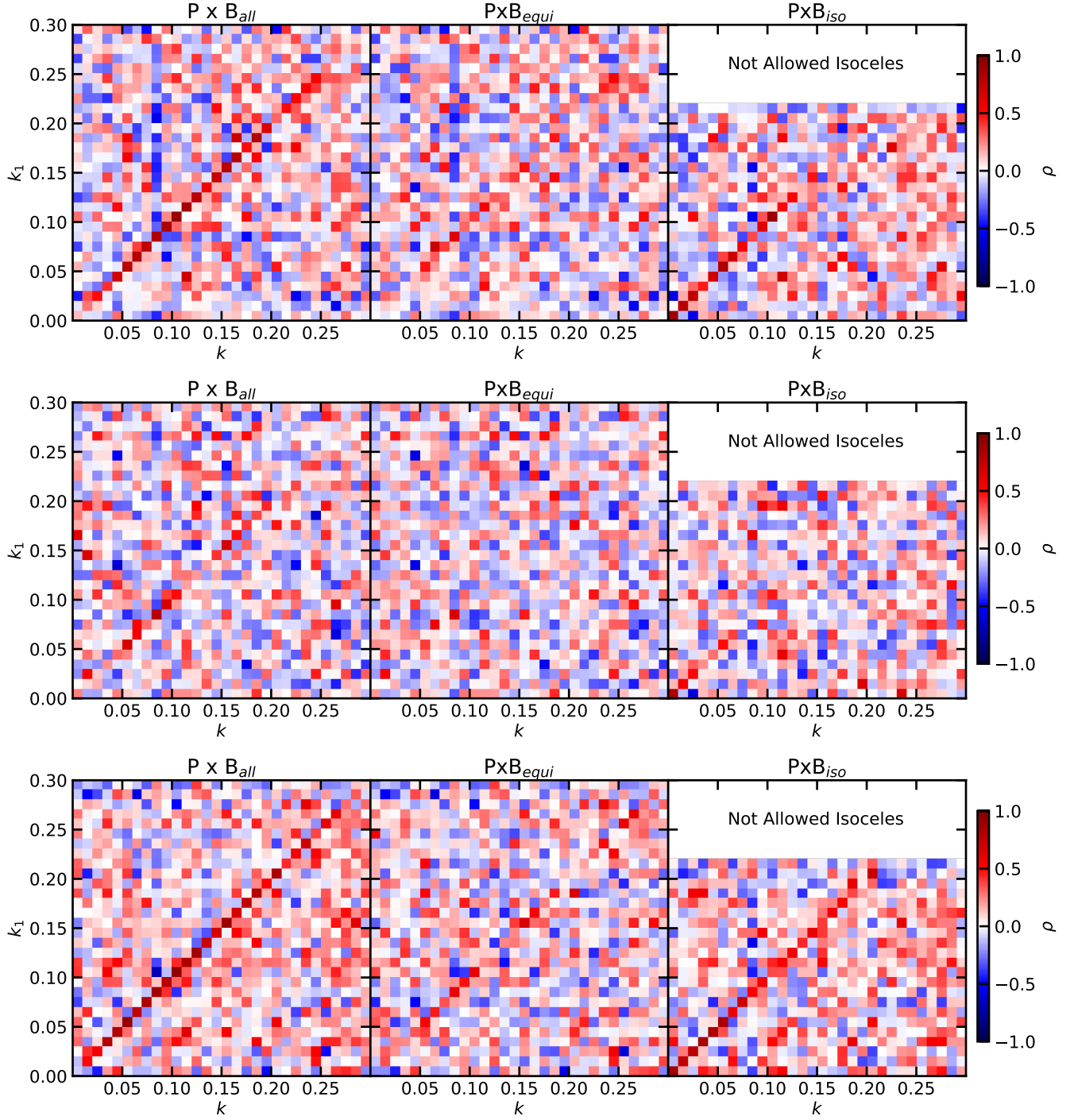


Figure 5. The bin-by-bin cross-correlation of the reduced bispectrum and power spectrum measurements for ABACUS LRG, ELG, and QSO samples. The left to right panel show different bispectrum configurations, respectively, all, equilateral, and isosceles.

APPENDIX A: TEMPLATES

The templates for power spectrum and bispectrum are validated in ?, and we briefly summarize the methods. These templates are used to qualitatively assess the location and magnitude of baryonic oscillations in power spectrum and bispectrum.

A1 Power spectrum

The fitting function or template for the power spectrum is given in (?), which assumes a general cold dark matter-baryon cosmology and corrects for the suppression of clustering on small scales, e.g., below the sound horizon. The power spectrum can be described as the multiplication of the primordial power spectrum and the square of the transfer function, which for a zero baryon cosmology is given

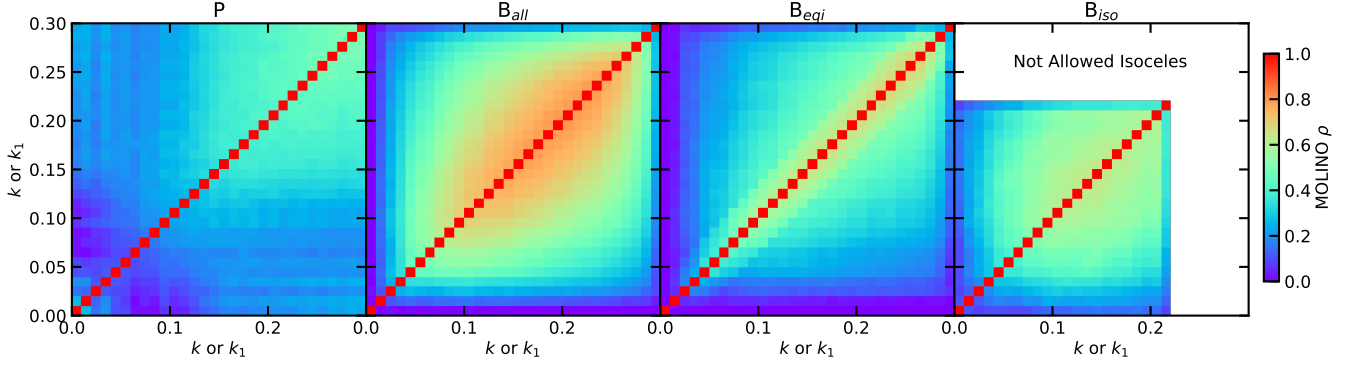


Figure 6. Bin-by-bin auto-correlation of Molino power spectrum and reduced bispectrum.

Table 1. BAO Constraints from LRG simulations

| Stat | Temp | Cov | $\langle \alpha \rangle$ | $\sigma(\alpha)$ | 4% | 96% |
|-----------|----------|----------|--------------------------|------------------|-------|-------|
| B | NASA | full | 0.957 | 0.010 | 0.005 | 0.010 |
| | NASA | diagonal | 0.954 | 0.008 | 0.003 | 0.007 |
| B | fiducial | full | 0.998 | 0.002 | 0.001 | 0.002 |
| | fiducial | diagonal | 0.997 | 0.001 | 0.001 | 0.003 |
| Reduced B | NASA | full | 0.961 | 0.009 | 0.005 | 0.012 |
| | NASA | diagonal | 0.958 | 0.009 | 0.007 | 0.013 |
| Reduced B | fiducial | full | 1.002 | 0.009 | 0.004 | 0.008 |
| | fiducial | diagonal | 1.002 | 0.008 | 0.008 | 0.013 |
| P | NASA | full | 0.959 | 0.005 | 0.002 | 0.006 |
| | NASA | diagonal | 0.958 | 0.005 | 0.003 | 0.006 |
| P | fiducial | full | 1.000 | 0.003 | 0.004 | 0.005 |
| | fiducial | diagonal | 1.001 | 0.004 | 0.004 | 0.00 |

Table 2. BAO Constraints from ELG simulations

| Stat | Temp | Cov | $\langle \alpha \rangle$ | $\sigma(\alpha)$ | 4% | 96% |
|-----------|----------|----------|--------------------------|------------------|-------|-------|
| B | NASA | full | 0.961 | 0.018 | 0.007 | 0.014 |
| | NASA | diagonal | 0.953 | 0.010 | 0.006 | 0.010 |
| B | fiducial | full | 0.998 | 0.001 | 0.001 | 0.002 |
| | fiducial | diagonal | 0.997 | 0.001 | 0.001 | 0.003 |
| Reduced B | NASA | full | 0.960 | 0.014 | 0.006 | 0.013 |
| | NASA | diagonal | 0.956 | 0.012 | 0.011 | 0.016 |
| Reduced B | fiducial | full | 1.002 | 0.011 | 0.004 | 0.010 |
| | fiducial | diagonal | 1.003 | 0.010 | 0.009 | 0.017 |
| P | NASA | full | 0.951 | 0.004 | 0.002 | 0.004 |
| | NASA | diagonal | 0.951 | 0.003 | 0.003 | 0.004 |
| P | fiducial | full | 1.000 | 0.003 | 0.003 | 0.004 |
| | fiducial | diagonal | 1.000 | 0.003 | 0.003 | 0.005 |

by,

$$T_0 = \frac{\ln(2e + 1.8q)}{\ln(2e + 1.8q) + C_0 q^2} \quad (\text{A1})$$

Table 3. BAO Constraints from QSO simulations

| Stat | Temp | Cov | $\langle \alpha \rangle$ | $\sigma(\alpha)$ | 4% | 96% |
|-----------|----------|----------|--------------------------|------------------|-------|-------|
| B | NASA | full | 0.962 | 0.012 | 0.006 | 0.012 |
| | NASA | diagonal | 0.961 | 0.012 | 0.003 | 0.008 |
| B | fiducial | full | 0.997 | 0.002 | 0.001 | 0.003 |
| | fiducial | diagonal | 0.996 | 0.002 | 0.001 | 0.003 |
| Reduced B | NASA | full | 0.965 | 0.012 | 0.004 | 0.015 |
| | NASA | diagonal | 0.962 | 0.012 | 0.007 | 0.018 |
| Reduced B | fiducial | full | 1.003 | 0.017 | 0.007 | 0.014 |
| | fiducial | diagonal | 1.000 | 0.014 | 0.013 | 0.021 |
| P | NASA | full | 0.963 | 0.008 | 0.002 | 0.006 |
| | NASA | diagonal | 0.961 | 0.008 | 0.003 | 0.008 |
| P | fiducial | full | 1.001 | 0.008 | 0.006 | 0.009 |
| | fiducial | diagonal | 1.001 | 0.008 | 0.007 | 0.011 |

where,

$$C_0 = 14.2 + \frac{731}{1 + 62.5q} \quad (\text{A2})$$

$$q = \left(\frac{k}{h\text{Mpc}^{-1}} \right)^2 \frac{\Theta_{\text{CMB}}^2}{\Omega_0 h} \quad (\text{A3})$$

where Θ is the temperature of the cosmic microwave background and Ω_0 is the total matter density. The damping on large scales due to baryons is described by,

$$\Gamma(k) = \Omega_0 h \left[a_\Gamma + \frac{1 - a_\Gamma}{1 + (0.43ks)^4} \right] \quad (\text{A4})$$

where

$$a_\Gamma = 1 - 0.328 \ln(431\Omega_0 h^2) \frac{\Omega_b}{\Omega_0} + 0.38 \ln(22.3\Omega_0 h^2) \left(\frac{\Omega_b}{\Omega_0} \right)^2 \quad (\text{A5})$$

where Ω_b represents the baryon density today.

A2 Bispectrum

Scoccimarro, Couchman, and Frieman (1998): bispectrum template with plane-parallel approx and damping factor (for nonlinear effects due to velocity dispersion).

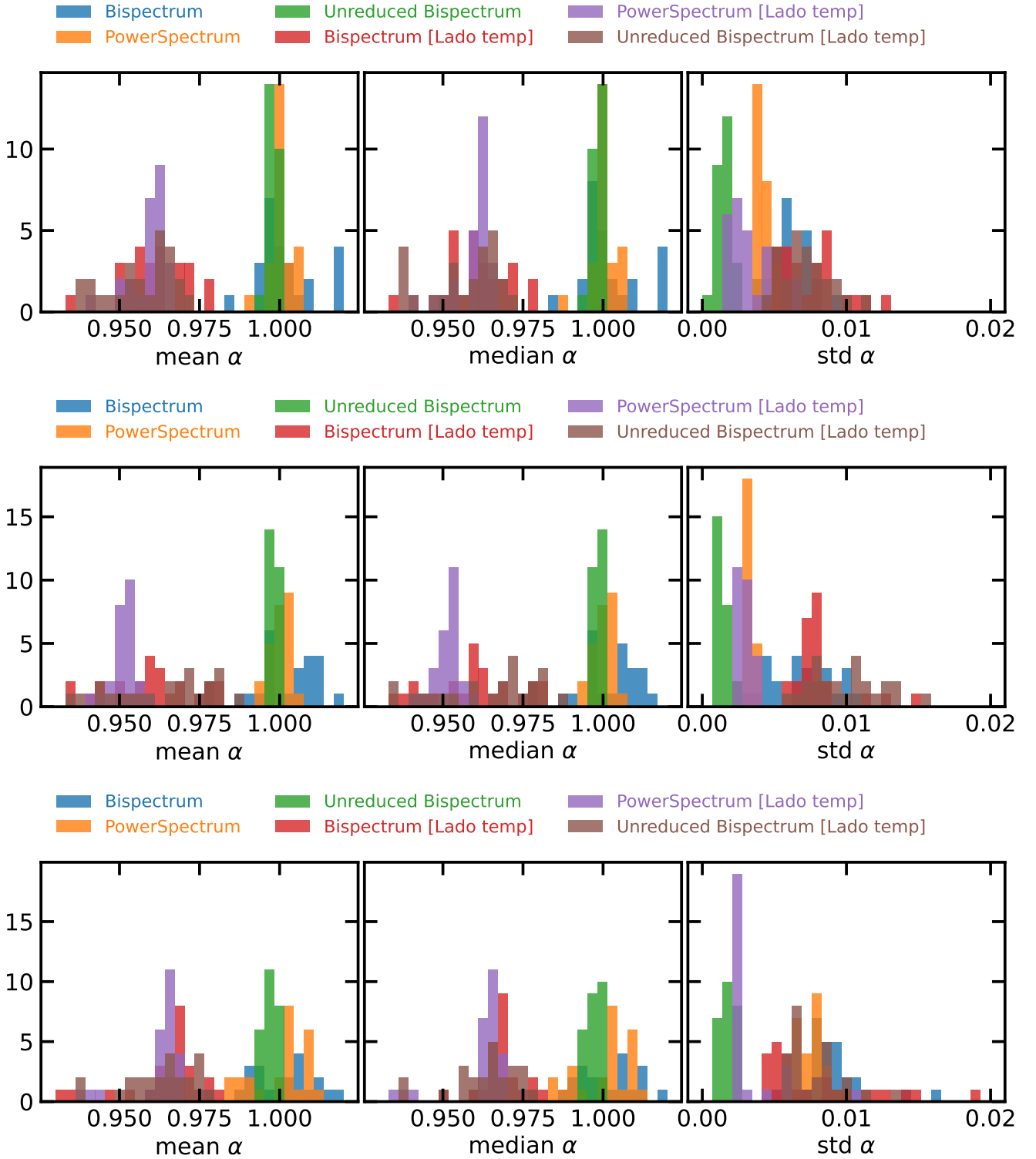


Figure 7. Mean, median, and standard deviation of BAO scale from 25 LRG (top), ELG (middle), and QSO (bottom) simulations.

This paper has been typeset from a \LaTeX file prepared by the author.

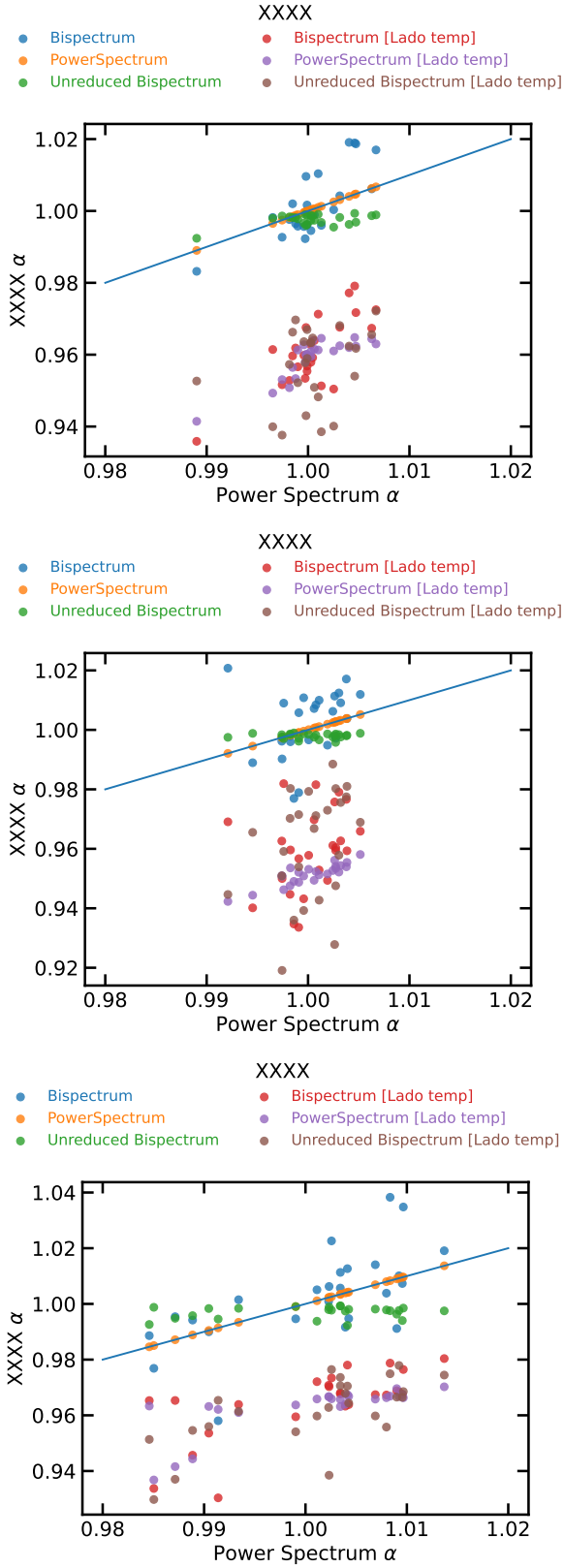


Figure 8. BAO scale from various measurements vs that of power spectrum for 25 LRG (top), ELG (middle), and QSO (bottom) simulations.